Nanoscale Advances

Accepted Manuscript

This article can be cited before page numbers have been issued, to do this please use: A. Sheardy, D. M. Arvapalli and J. Wei, *Nanoscale Adv.*, 2020, DOI: 10.1039/D0NA00069H.

ROYAL SOCIETY OF CHEMISTRY

rsc.li/nanoscale-advances

View Article Online
DOI: 10.1039/D0NA00069H

COMMUNICATION

Novel microwave synthesis of near-metallic copper sulfide nanodiscs with size control: experimental and DFT studies of charge carrier density

Received 00th January 20xx,
Accepted 00th January 20xx

DOI: 10.1039/x0xx00000x

Alex T. Sheardy,[a] Durga M. Arvapalli,[a] Jianjun Wei*[a]

A simple unprecedented microwave synthesis of size controllable copper sufide (CuS) nanodiscs is reported. Experimental results and density functional theory (DFT)-calculated results determine the charge carriers densities on the order of 10^{21} cm^{-3} with an effective mass of 0.3m_e, resulting in near-metallic properties.

Copper sulfide (Cu_xS, $1 \leq x \leq 2$) nanoparticles have recently been the focus of a variety of optical-based studies, including: bioimaging/detection,[1, 2] photothermal therapy,[3, 4] photovoltaics,[11] and photocatalysis.[12, 13] The majority of these studies are based on the plasmonic near-infrared absorption band, which has been explicitly studied both experimentally[9, 14, 15] and theoretically.[16-18] The plasmon absorption arises from intrinsic p-doping that is dependent on the stoichiometric ratio of Cu:S; increased sulfur content results in increased p-doping and therefore a stronger and higher energy plasmon absorption.[5, 6, 9, 19-24] This results in more controllability of the plasmon in comparison to traditional noble metal nanoparticles, as the charge carrier density can be modified in semiconductor plasmons in addition to size and morphology.[25] Stoichiometric CuS (x=1, covellite) is the most heavily doped of the copper sulfides, thus exhibiting the strongest plasmon absorption and of the most interest for these potential applications.[14, 15]

Despite the myriad potential applications for CuS NPs, most of the syntheses used are not ideal for wide-spread use. A summary of some of the various synthetic methods used to synthesize Cu_xS NPs of varying stoichiometry is gathered in Table S1. Many of these reactions require temperatures on the order of 150-200 °C and/or multistep preparation of precursors. Some hydrothermal syntheses at lower temperature (90 °C) have been performed, but the concentration used in these reactions was 1 mM, making this prohibitive for commercial applications.

[a] Department of Nanoscience, Joint School of Nanoscience and Nanoengineering, University of North Carolina at Greensboro, Greensboro, NC 27401, USA. *j_wei@uncg.edu, Tel: 1-336-285-2859. 2907 E. Gate City Blvd, Greensboro, NC 27401, USA.

Electronic Supplementary Information (ESI) available: [Experimental procedure and characterization methods]. See DOI: 10.1039/x0xx00000x

Copper sulfide NPs have been synthesized using microwave synthesis, however these works generally resulted in micron-sized particles with nanoscale features. Kim *et al.* did synthesize 13 nm CuS nanodiscs, but the procedure required multiple steps and the reaction was not explored in depth.[20]

Microwave synthesis is an emerging technique used in both organic[26] and inorganic[27] synthesis that could potentially replace conventional heating in many processes and allow for more efficient synthesis. Microwave-assisted synthetic methods show many advantages over traditional heating, including reduced reaction times, faster/more uniform heating, increased reproducibility, and simpler reaction setups. In a simple sense, microwave heating functions by causing molecular rotations which result in molecular friction and therefore heat. Further, since the microwaves can penetrate through the solvent, heating can occur in the entire reaction simultaneously, vs. conventional heating which is dependent on external heating and stirring to achieve thermal equilibrium. Finally, traditional heating methods can require high temperatures and techniques like hot injection to achieve reproducible nanoparticle size, but the rapid heating of microwave reactions eliminates the need for complicated synthetic techniques.[26, 27] For these reasons, we aim to provide a more comprehensive study on the microwave synthesis of plasmonic CuS nanoparticles.

Further, while many of the proposed applications for CuS NPs are based on the electronic properties of the NPs, these properties remain poorly treated. As mentioned above, copper sulfides are intrinsically p-doped, meaning the charge carriers are mainly holes. The density of charge carriers is of particular interest, as it affects both the energy of the plasmon and the conductivity. Calculation of the charge carrier density is often performed using the Drude model (Eq. 1, 2, see discussion), which has dependence on both the shape of the nanoparticle and the effective mass of the charge carriers.[7, 9, 15, 20, 23, 24] Often in literature, the shape factor is assumed to be that of a spherical particle (L = 1/3), regardless of the actual shape of the particle. The effective mass of holes in Cu_2S has been reported in literature as $0.8m_e$,[18] however the effective mass for

View Article Online
DOI: 10.1039/D0NA00069H

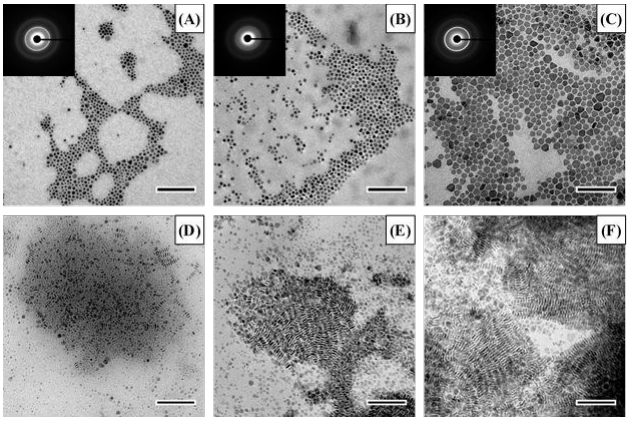

Figure 1. Representative TEM micrographs of CuS NPs synthesized for 5 (A,D), 10 (B,E), or 15 (C,F) minutes either parallel (A-C) or perpendicular (D-F) to the carbon support film. The insets on the micrographs show the electron diffraction pattern, and the scale bar on all images is 100 nm.

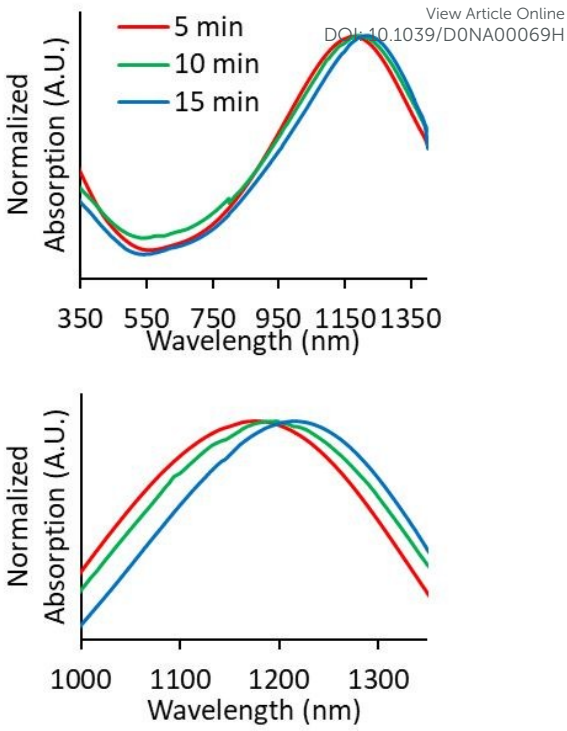

Figure 2: UV-Vis-NIR absorption spectra of CuS synthesized with reaction times of 5 (Red), 10 (Green), and 15 minutes (Blue). The spectra have been normalized for comparison, and both the entire spectra (top) and plasmon absorption (bottom) are shown. The peak absorptions occur at 1176, 1197, and 1215 nm, respectively.

stoichiometric CuS has not been theoretically studied and rather is assumed to be the same as Cu_2S. This assumption is unlikely valid based on the results of the computational study by Lukashev *et al.*, which shows that Cu_2S is a traditional semiconductor, while the introduction of additional sulfur atoms introduces more metallic character.[18] A review by Kriegel *et al.* on plasmonic semiconductors presents an experimentally reported CuS effective mass of $0.55m_e$, however these experiments were based on an experimental study of $Ba_{1-x}K_xCuSF$, making it erroneous to attribute this value to pure CuS.[6, 19, 28] As such, the authors are unaware of any experimental or theoretical studies that have determined the effective mass for carriers in pure stoichiometric CuS. For these reasons, we have combined experimental results with density functional theory (DFT)-calculated results to better determine both an experimental and theoretical charge carrier density in CuS nanoparticles, along with an appropriate effective mass for the charge carriers.

The synthesis procedure is provided in SI. TEM images of the synthesized CuS NPs are given in Figure 1 both parallel (A-C) and perpendicular (D-F) to the support film. As can be seen from the images, there is an obvious increase in the diameter of the particles with increasing reaction time, and multiple morphologies including circles, triangles and hexagons are present. The insets on Figure 1 show the electron diffraction pattern, indicating the crystalline nature of the particles. Specifically, the bright ring in all samples corresponds to the $(2\bar{1}0)$ plane, with a lattice spacing of 1.88 Å. From Figure 1D-F, it can be seen that the particles are discs, which is consistent with the expected hexagonal crystal structure. Size distributions for both the diameter and height of the particles are given in Fig S1, and there is a clear increase in both dimensions with increasing reaction time. The size data is also summarized in Table 1.

FTIR spectroscopy was used to confirm the presence of the oleylamine capping agent (Fig S2A), and the agreement between pure oleylamine and the CuS NPs can be clearly seen. TGA between 100-800 °C shows similar structure between all reaction times, with two main mass losses at ~250 and ~450 °C (Fig S2B). The first of these losses corresponds to ~30% of the mass and is due to the loss of sulfur and formation of higher copper stoichiometries.[29] The second loss is approximately 40% of the initial mass and is attributed to the loss of the oleylamine capping agent. XPS was performed to verify the expected 1:1 stoichiometry for CuS (Fig S2C). From these experiments, the major elements present are copper, sulfur, carbon, nitrogen, and oxygen. The carbon and nitrogen are expected from the oleylamine capping agent, while the oxygen may be due to surface contamination. Table S2 lists the Cu and S content for each sample, and the materials do present an approximate 1:1 relationship. The relatively low elemental content of each of these elements (2-8% each) and deviations from 1:1 stoichiometry are due to a high carbon content (~75-80%) from the capping agent and the relatively shallow probe depth of the technique. High resolution scans of the Cu L-edge give a single peak for the p3/2 signal at ~933.3 eV and a single peak for the p1/2 signal at ~953.1 eV (Fig. S3D). For the S L-edge, a single peak at ~163.5 eV is observed (Fig. S3E).

X-Ray Diffraction was performed to verify that the crystal structure of the synthesized nanodiscs matches the expected structure for stoichiometric CuS (Fig S3). As can be seen, the experimental data for all synthesized samples show good agreement with the predicted diffraction pattern shown in black. Taken together the FTIR, TGA, XRD and XPS data confirm the

View Article Online
DOI: 10.1039/D0NA00069H

synthesis of stoichiometric CuS capped with oleylamine, with no major differences between different reaction times, excepting size/aspect ratio.

UV-Vis-NIR spectra were measured (Figure 2), and it can be seen that there is a red shift of the NIR plasmon peak with increasing reaction time. Based on this plasmon peak, it is possible to calculate the density of charge carriers (holes), n_h, according to the Drude model and Eqs. 1-2. [7, 9, 15, 20, 23, 24] In these equations, ω_{sp} is the surface plasmon frequency, ω_p is the bulk plasmon frequency, ε_m is the dielectric constant of the media ($CHCl_3$, 4.81), γ is the plasmon linewidth, L is the shape factor, e is the charge of an electron, m_h is the effective mass of the holes, and ε_0 is the free space permittivity. In the calculations that follow, ω_{sp} and γ are taken from the position and FWHM of the plasmon resonance, respectively. The shape factor for an oblate ellipsoid can be found using Eq. 3, and for disc-like particles it is assumed that $L_x = L_y < L_z$ ($r_1 = r_2 < r_3$).[30] Finally, an effective hole mass of $0.8m_e$ was used, based on previous literature.[9, 24] These calculations result in hole densities of 1.25, 1.24, and 1.41 × 10^{22} cm^{-3} for 5, 10 and 15 minute reactions, respectively. For comparison, gold and copper have electron densities of 5.9 and 8.4 × 10^{22} cm^{-3}, respectively, so the synthesized CuS NPs are approaching near-metallic levels of charge carriers. All of the data used in these calculations is summarized in Table 1.

$$\omega_{sp} = \sqrt{\frac{\omega_p^2}{1 + (\frac{1}{L} - 1)\varepsilon_m} - \gamma^2} \quad (1)$$

$$\omega_p = \sqrt{\frac{n_h e^2}{m_h \varepsilon_0}} \quad (2)$$

$$L_i = \frac{r_1 r_2 r_3}{2} \int_0^\infty \frac{ds}{(s + r_i^2)\sqrt{(s + r_1^2)(s + r_2^2)(s + r_3^2)}} \quad (3)$$

Density functional theory (DFT) calculations of the total energy, density of states, and band structure were calculated using Quantum Espresso,[31] following the methodology of Morales-Garcia *et al*.[16] Specifically, the calculations were performed using the generalized gradient approximation (GGA), with a projector-augment wave (PAW) all-electron description[32, 33] and Perdew, Burke, and Ernzerhof (PBE) exchange-correlation functional.[34] Calculations were performed using a Monkhorst-Pack[35] grid of k-points (10 x 10 x 2), with a plane-wave cutoff of 560 eV. For convergence, a consecutive total energy difference of less than 10^{-4} eV was required. Since DFT is known to underestimate the bandgap, the Dudarev simplified rotationally invariant form of DFT+U was used.[36] Values of U (6 eV) and J (1 eV) were chosen based on the results from Morales-Garcia *et al*, giving an effective U of 5 eV.[16]

A number of different copper sulfide stoichiometries have been studied in terms of the carrier effective mass, charge carrier density, and band gap; these data have been collected in Table 2. Cu_2S has been shown to be purely semiconducting, and therefore has insufficient charge carriers to support a plasmon.[9, 18] Increasing sulfur content results in increased charge carrier densities, with the charger carrier density for CuS being approximately one order of magnitude higher than the less heavily doped stoichiometries. Specifically, previous literature has reported CuS hole densities in the range of 0.5 – 1.6 × 10^{22} cm^{-3}, of similar order to those report in this work.[5, 6, 20-24] It should be noted that most of these calculations are dependent on the effective mass of the charge carriers (holes), but these values have only been computationally reported for Cu_2S, and other studies assume that the mass does not change significantly. The near-metallic nature of CuS[23] suggests that the effective mass of the carrier should be different from that of purely semiconducting Cu_2S. For this, values of 0.55, 0.8, and $1m_e$ have been used, but the former of these comes from an experiment using $Ba_{1-x}K_xCuSF$,[19] while the latter values are assumptions.

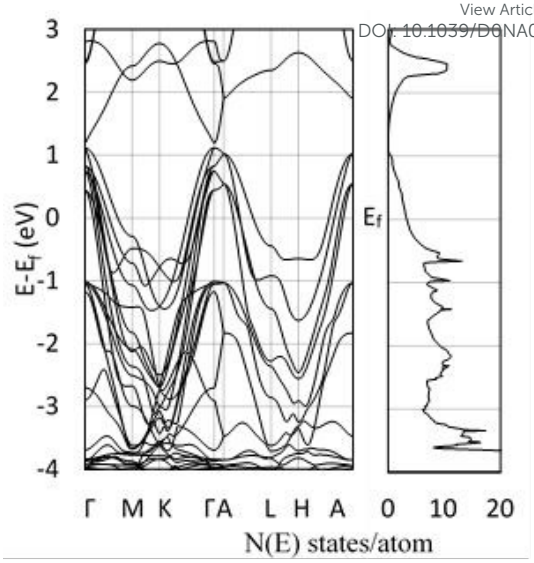

Figure 3. DFT-calculated band structure (left) and density of states (right) using DFT+U (Ueff=5). Energies are relative to the Fermi energy, and both figures share the same y-axis values.

In order to verify the experimental charge carrier density, a density functional theory (DFT) calculation of the band structure and density of states (DOS) was performed (Figure 3), following the methodology of Morales-Garcia *et al*.[16] Using DFT+U, the band structure and DOS of bulk CuS were calculated (Figure 3) and show good agreement with Morales-Garcia's calculations. From simple solid state physics, the number of charge carriers

Table 1. Summary of data used for charge carrier density calculation.

Time (min)	Diameter (nm)	Height (nm)	L_x	λ (nm)	γ (eV)	$\hbar\omega_{sp}$ (eV)	$\hbar\omega_p$ (eV)	n_h (10^{22} cm^{-3})
5	6.5 ± 1.9	3.3 ± 0.5	0.239	1176 ± 2.6	0.461	1.05	4.65	1.25
10	8.5 ± 2.3	4.2 ± 0.7	0.235	1197 ± 7.6	0.454	1.04	4.62	1.24
15	11.6 ± 3.2	4.5 ± 0.7	0.202	1215 ± 27.5	0.411	1.02	4.92	1.41

View Article Online DOI: 10.1039/D0NA00069H

Table 2. Summary of previously used/reported values for carrier effective mass, charge carrier density and band gap for multiple Cu_xS stoichiometries. The results from this work are also included.

Stoichiometry	Carrier Effective Mass (m_e)	Charge Carrier Density (cm^{-3})	Band Gap (eV)
Cu_2S[5, 14]	0.8	-	0.6, 2.4
$Cu_{1.94}S$ - $Cu_{1.98}S$[5-10]	0.8	0.7 - 1.3 x 10^{21}	1.53
$Cu_{1.94}S$ - $Cu_{1.8}S$ (Theoretical)[18]	-	0.8 - 2.4 x 10^{21}	0.55
$Cu_{1.8}S$[5, 6, 10]	0.8	3.0 - 4.6 x 10^{21}	1.46, 2.55
$Cu_{1.4}S$[5, 21]	0.8	5.88 x 10^{21}	2.5
CuS[2, 5, 6, 10, 20-24]	0.55-1	0.5 - 1.6 x 10^{22}	1.48, 2.58
CuS (This work)	0.3	9.8 x 10^{21} (Theoretical) 4.7-5.27 x 10^{21} (Experimental)	N/A

(*N*) is given by Eq. 4, where *f(E)* is the Fermi-Dirac distribution and *g(E)* is the density of states.[37] At 0 K, the Fermi-Dirac distribution for holes would simplify to either 0 ($E < E_f$) or 1 ($E > E_f$). While this assumption is only completely accurate at 0 K, at higher temperatures the distribution of charge carriers will change, but the total density should remain relatively unchanged. Further, seeing as the Fermi energy is within the conduction band, only the holes within that same band are likely to contribute to charge carrying in the plasmon, as holes in higher bands would be too high energy. Taking these assumptions together, Eq. 4 can be simplified to Eq. 5, where E_c is the top of the conduction band and V is the unit cell volume. Performing this calculation results in a calculated ~2 holes per unit cell, or $n_h = 9.81 \times 10^{21}$ cm^{-3}. This computationally derived result shows good agreement both with previous literature and the present results. Specifically, the value of two holes per unit cell is consistent with the prediction of Conejeros *et al*., based on the expected number of electrons and the number of states available.[38] Work by Mazin also shows similar results of 1/3 of a hole per Cu, combined with the 6 copper atoms per unit cell gives a total of two holes per unit cell.[39]

$$N(E) = \int f(E)g(E)dE \quad (4)$$

$$n_h V = N_h = \int_{E_f}^{E_c} g(E)dE \quad (5)$$

The DFT-calculated charge density is of similar order, but slightly lower than the experimentally calculated value. One likely source for this discrepancy is an over-estimation of the value of γ, due to experimental broadening of the peak. Additionally, the dielectric constant used was for chloroform, while the oleylamine capping agent likely changes the effective dielectric constant around the NPs. Finally, the largest source of discrepancy between experiment and theory could come from the choice of the effective hole mass as $0.8m_e$. As previously discussed, the prior reported values for the hole mass in CuS do not come from pure samples, or is assumed to be the same as Cu_2S. For this reason, the effective hole mass was calculated in the Γ-M direction around the Fermi energy using Eq. 6. Performing this calculation results in an effective hole mass of $0.3m_e$. The Γ-M direction was selected based both on the work of Lukashev *et al.*[18] and the fact that this represents the same transverse direction the plasmon oscillates in. As a note; the Γ-K direction was also tested, to ensure that there were no significantly different effective masses. The calculated effective mass is consistent with Lukashev's calculated electron effective mass for Cu_2S, a result that is not unexpected. For a metal at reasonable temperatures, the narrow spread of the Fermi-Dirac distribution should result in electrons and holes having similar effective masses. Using this effective mass results in experimental charge carrier densities of 4.70, 4.64 and 5.27 × 10^{21} cm^{-3}, which are approximately half of the predicted value of 9.81 × 10^{21} cm^{-3}. This effective mass can be considered as a lateral effective mass; the transverse effective mass calculated at the Γ point using the Γ-A direction is significantly larger with $m_h^* = 3.7m_e$ and $m_e^* = 0.83m_e$. Combined with a calculated energy gap of 1.45 eV in the z-direction, it is not expected that there will be sufficient carriers with small enough effective mass to support an out-of-plane plasmon. The band structures in the Γ-A and Γ-M direction used for these calculations can be found in Fig. S4.

$$E = \frac{\hbar^2 k^2}{2m_h} \quad (6)$$

In conclusion, a new simple size-controlled microwave synthesis method for oleylamine-capped CuS nanodiscs has been developed. The particles have undergone multiple characterization techniques to accurately determine the structure and confirm that the only differences made by reaction time are the size of the disc-like NPs and resulting plasmon absorption. Further, using a conventional effective hole mass of $0.8m_e$, charge carrier densities 1.2-1.4 × 10^{22} cm^{-3} were obtained, while density functional theory was used to determine a predicted charge carrier density of 9.81 × 10^{21} cm^{-3}. Using the calculated band structure around the Fermi energy resulted in a lower effective hole mass of $0.3m_e$, closer to that predicted for electrons in less heavily doped copper sulfides. Finally, using this calculated effective mass, the experimental charge carrier densities were recalculated as 4.7-5.3 × 10^{21} cm^{-3}, approximately half of the predicted value.

The authors acknowledge the support from NSF grants (1511194 and 1832134). This work was performed at the JSNN, a member of South Eastern Nanotechnology Infrastructure Corridor (SENIC) and National Nanotechnology Coordinated Infrastructure (NNCI), which is supported by the National Science Foundation (ECCS-1542174).

Conflicts of interest

There are no conflicts to declare.

Notes and references

1. K. Ding, J. Zeng, L. Jing, R. Qiao, C. Liu, M. Jiao, Z. Li and M. Gao, *Nanoscale*, 2015, **7**, 11075-11081.
2. G. Ku, M. Zhou, S. Song, Q. Huang, J. Hazle and C. Li, *ACS Nano*, 2012, **6**, 7489-6496.
3. M. Zhou, J. Li, S. Liang, A. K. Sood, D. Liang and C. Li, *ACS Nano*, 2015, **9**, 7085-7096.
4. M. Zhou, R. Zhang, M. Huang, W. Lu, S. Song, M. P. Melancon, M. Tian, D. Liang and C. Li, *J Am Chem Soc*, 2010, **132**, 15351-15358.
5. I. Grozdanov and M. Najdoski, *Journal of Solid State Chemistry*, 1995, **114**, 469-475.
6. S. W. Hsu, C. Ngo and A. R. Tao, *Nano Lett*, 2014, **14**, 2372-2380.
7. S.-W. Hsu, W. Bryks and A. R. Tao, *Chem. Mater.*, 2012, **24**, 3765-3771.
8. S.-W. Hsu, K. On and A. R. Tao, *Journal of the American Chemical Society*, 2011, **133**, 19072-19075.
9. J. M. Luther, P. K. Jain, T. Ewers and A. P. Alivisatos, *Nat Mater*, 2011, **10**, 361-366.
10. P. Parreira, G. Lavareda, A. Amaral, A. M. Botelho do Rego, O. Conde, J. Valente, F. Nunes and C. Nunes de Carvalho, *Journal of Alloys and Compounds*, 2011, **509**, 5099-5104.
11. H. Lee, S. W. Yoon, E. J. Kim and J. Park, *Nano Lett*, 2007, **7**, 778-784.
12. Y. Kim, K. Y. Park, D. M. Jang, Y. M. Song, H. S. Kim, Y. J. Cho, Y. Myung and J. Park, *J Phys Chem C*, 2010, **114**, 22141-22146.
13. C. Ratanatawanate, A. Bui, K. Vu and K. J. Balkus, *J. Phys. Chem. C*, 2011, **115**, 6175-6180.
14. M. C. Brelle, C. L. Lorres-Martinez, J. C. McNulty, R. K. Mehra and J. Z. Zhang, *Pure Appl. Chem.*, 2000, **72**, 101-117.
15. Y. Zhao, H. Pan, Y. Lou, X. Qui, J. Zhu and C. Burda, *J Am Chem Soc*, 2009, **131**, 4253-4261.
16. A. Morales-Garcia, A. L. Soares, Jr., E. C. Dos Santos, H. A. de Abreu and H. A. Duarte, *J Phys Chem A*, 2014, **118**, 5823-5831.
17. L. Xiao, J. Wu, J. Ran, Y. Liu, W. Qiu, F. Lu, F. Shao, D. Tang and P. Peng, *AIP Advances*, 2016, **6**, 085122.
18. P. Lukashev, W. R. L. Lambrecht, T. Kotani and M. van Schilfgaarde, *Phys. Rev. B*, 2007, **76**, 195202.
19. R. Kykyneshi, PhD Dissertation, Oregon State University, 2007.
20. M. R. Kim, H. A. Hafez, X. Chai, L. V. Besteiro, L. Tan, T. Ozaki, A. O. Govorov, R. Izquierdo and D. Ma, *Nanoscale*, 2016, **8**, 12946-12957.
21. L. Liu, H. Zhong, Z. Bai, T. Zhang, W. Fu, L. Shi, H. Xie, L. Deng and B. Zou, *Chemistry of Materials*, 2013, **25**, 4828-4834.
22. M. Liu, X. Xue, C. Ghosh, X. Liu, Y. Liu, E. P. Furlani, M. T. Swihart and P. N. Prasad, *Chemistry of Materials*, 2015, **27**, 2584-2590.
23. Y. Xie, L. Carbone, C. Nobile, V. Grillo, S. D'Agostino, F. D. Sala, C. Giannini, D. Altamura, C. Oelsner, C. Kryschi and P. D. Cozzoli, *ACS Nano*, 2013, **7**, 7352-7369.
24. Y. Xie, A. Riedinger, M. Prato, A. Casu, A. Genovese, P. Guardia, S. Sottini, C. Sangregorio, K. Miszta, S. Ghosh, T. Pellegrino and L. Manna, *J Am Chem Soc*, 2013, **135**, 17630-17637.
25. P. K. Jain, K. Manthiram, J. H. Engel, S. L. White, J. A. Faucheaux and A. P. Alivisatos, *Angew Chem Int Ed Engl*, 2013, **52**, 13671-13675.
26. C. O. Kappe, *Angew Chem Int Ed Engl*, 2004, **43**, 6250-6284.
27. I. Bilecka and M. Niederberger, *Nanoscale*, 2010, **2**, 1358.
28. I. Kriegel, F. Scotognella and L. Manna, *Physics Reports*, 2017, **674**, 1-52.
29. E. Godočíková, P. Baláž, J. M. Criado, C. Real and E. Gock, *Thermochimica Acta*, 2006, **440**, 19-22.
30. W. L. Barnes, *Am. J. Phys.*, 2016, **84**, 593-601.
31. P. Giannozzi, S. Baroni, N. Bonini, M. Calandra, R. Car, C. Cavazzoni, D. Ceresoli, G. L. Chiarotti, M. Cococcioni, I. Dabo, A. Dal Corso, S. de Gironcoli, S. Fabris, G. Fratesi, R. Gebauer, U. Gerstmann, C. Gougoussis, A. Kokalj, M. Lazzeri, L. Martin-Samos, N. Marzari, F. Mauri, R. Mazzarello, S. Paolini, A. Pasquarello, L. Paulatto, C. Sbraccia, S. Scandolo, G. Sclauzero, A. P. Seitsonen, A. Smogunov, P. Umari and R. M. Wentzcovitch, *J Phys Condens Matter*, 2009, **21**, 395502.
32. P. E. Blöchl, *Phys. Rev. B*, 1994, **50**, 17953-17979.
33. G. Kresse and D. Joubert, *Phys. Rev. B*, 1999, **59**, 1758-1775.
34. J. P. Perdew, K. Burke and M. Ernzerhof, *Phys. Rev. Lett.*, 1996, **77**, 3865-3868.
35. H. J. Monkhorst and J. D. Pack, *Phys. Rev. B*, 1976, **13**, 5188-5192.
36. S. L. Dudarev, G. A. Botton, S. Y. Savrasov, C. J. Humphreys and A. P. Sutton, *Phys. Rev. B*, 1998, **57**, 1505-1509.
37. C. Kittel, *Introduction to Solid State Physics, 8th Edition*, Wiley, 2004.
38. S. Conejeros, P. Moreira Ide, P. Alemany and E. Canadell, *Inorg Chem*, 2014, **53**, 12402-12406.
39. I. I. Mazin, *Physical Review B*, 2012, **85**, 115133.

View Article Online
DOI: 10.1039/D0NA00069H

TOC Only

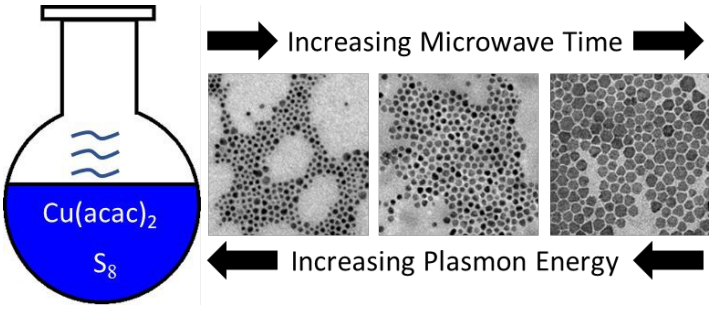

A simple one-step microwave-assisted synthesis of CuS nanodiscs with size and optical property control.